Synthesis, Structures, Dynamics, and Olefin Polymerization Behavior of Group 4 Metal $(pyCAr_2O)_2M(NR_2)_2$ Complexes Containing Bidentate Pyridine−Alkoxide Ancillary Ligands

Il Kim, Yasushi Nishihara, and Richard F. Jordan*

Department of Chemistry, The University of Iowa, Iowa City, Iowa 52242

Robin D. Rogers

Department of Chemistry, The University of Alabama, Tuscaloosa, Alabama 35487

Arnold L. Rheingold and Glenn P. A. Yap

Department of Chemistry, The University of Delaware, Newark, Delaware 19716

Received March 24, 1997[⊗]

The reaction of 2-lithiopyridine and the appropriate diarylketone followed by hydrolysis yields $pyCAr_2OH$ pyridine−alcohols (**1a**, Ar = 4-^{t}Bu−C_6H_4; **1b**, $pyCAr_2OH$ = 2-pyridyl-9-fluorenol; **1c**, Ar = 3-CF_3−C_6H_4; **1d**, Ar = 4-Ph−C_6H_4; **1e**, Ar = 4-NEt_2−C_6H_4; **1f**, $pyCAr_2$-OH = 1-(2-pyridyl)-1-dibenzosuberol; **1g**, Ar = 3,5-$(CF_3)_2$−C_6H_3). The reaction of $Ti(NMe_2)_4$ with 2 equiv of **1a**−**g** yields $(pyCAr_2O)_2Ti(NMe_2)_2$ (**2a**−**g**) and NMe_2H. The reaction of $Zr(NMe_2)_4$ with 2 equiv of **1a**,**b**,**e** yields $(pyCAr_2O)_2Zr(NMe_2)_2$ (**3a**,**b**,**e**), while similar reactions with **1c**,**d** yield mixtures of $(pyCAr_2O)_xZr(NMe_2)_{4-x}$ (x = 1−3) species. $\{pyC(3\text{-}CF_3\text{−}C_6H_4)_2O\}_3Zr(NMe_2)$ (**4c**) and $\{pyC(4\text{-}NEt_2\text{−}C_6H_4)_2O\}_4Zr$ (**5e**) are prepared from $Zr(NMe_2)_4$ and 3 equiv of **1c** or 4 equiv of **1e**, respectively. The reaction of $Hf(NMe_2)_4$ with 2 equiv of **1a**,**e** yields $(pyCAr_2O)_2Hf(NMe_2)_2$ (**6a**,**e**), while reaction with 3 equiv of **1b**,**c** yields $(pyCAr_2O)_3Hf(NMe_2)$ (**7b**,**c**). X-ray crystallographic analyses establish that **2b**, **2e**, and **3a** adopt distorted octahedral structures with a *trans*-O, *cis*-py, *cis*-amide arrangement of ligands. NMR data show that $(pyCAr_2O)_2M(NMe_2)_2$ complexes adopt the same structure in solution but undergo inversion of configuration at the metal with racemization barriers ($\Delta G^{\ddagger}$ (racemization)) in the range of 12−14 kcal/mol. Treatment of $(pyCAr_2O)_2M(NMe_2)_2$ complexes with $Al(^iBu)_3$ and methylalumoxane (MAO) yields active, multisite ethylene polymerization catalysts.

Introduction

Recently, we described the synthesis of new group 4 metal alkyl complexes of the general form $(Ox)_2MR_2$ and $(pyCR_2O)_2MR_2$ which contain quinolinolato or pyridine−alkoxide ancillary ligands (Chart 1).[1] These species adopt chiral C_2-symmetric structures with a *trans*-O, *cis*-pyridine, *cis*-alkyl ligand arrangement but undergo inversion of configuration at the metal (i.e., Λ/Δ isomerization) on the NMR time scale. The corresponding mono(alkyl) $(Ox)_2MR^+$ and $(pyCR_2O)_2MR^+$ cations were also prepared and are active catalysts for the polymerization of ethylene and, in some cases, α-olefins. These species adopt distorted square pyramidal structures which are stereorigid in some cases and in which the ligand arrangement is dictated by the π-donor properties of the alkoxide ligands (Chart 1). It is of interest to investigate the influence of the $pyCR_2O^-$ ligand structure on the stereochemical rigidity and reactivity of $(pyCR_2O)_2MR_2$ and $(pyCR_2O)_2MR^+$ species in order to eventually develop stereoselective catalysts.

Chart 1

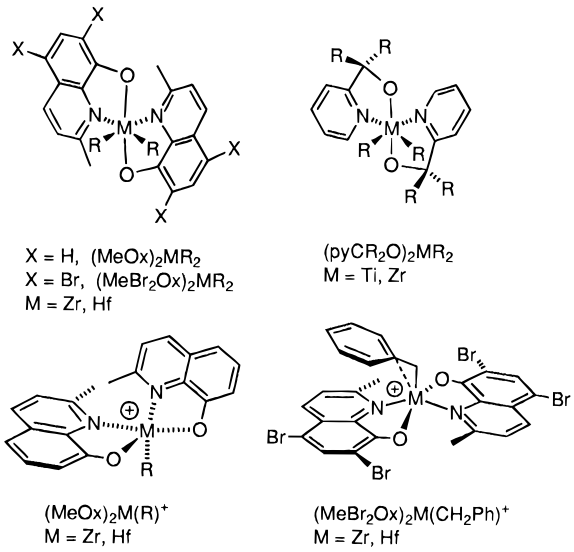

In other work, we have shown that chiral *ansa*-metallocene amide complexes $^{ch}Cp_2M(NR_2)_2$, such as *rac*-(ethylenebis(tetrahydroindenyl))$Zr(NMe_2)_2$ and *rac*-$Me_2Si(indenyl)_2Zr(NMe_2)_2$, may be prepared efficiently by amine elimination reactions of $M(NR_2)_4$ complexes and appropriate *ansa*-cyclopentadiene reagents.[2] These species are converted to $^{ch}Cp_2M(R)^+$ cations, which are

[⊗] Abstract published in *Advance ACS Abstracts,* June 15, 1997.

(1) (a) Bei, X.; Swenson, D. C.; Jordan, R. F. *Organometallics* **1997**, *16*, 3282. This paper contains an extensive listing of references dealing with other recent studies of non-Cp_2M olefin polymerization catalysts. (b) Tsukahara, T.; Swenson, D. C.; Jordan, R. F. *Organometallics* **1997**, *16*, 3303. (c) Tsukahara, T.; Lubben, T.; Swenson, D. C.; Young, V. G., Jr.; Jordan, R. F. Manuscript in preparation.

S0276-7333(97)00236-7 CCC: $14.00

active for olefin polymerization, via alkylation with AlR_3 reagents and subsequent reaction with MAO, $B(C_6F_5)_3$, HNR_3^+ reagents, or CPh_3^+ reagents.[3] The simplicity and success of this approach to metallocene catalysis suggested that a similar strategy would facilitate the investigation of structure/reactivity relationships in $(pyCR_2O)_2MR_2$ and $(pyCR_2O)_2MR^+$ systems. Here, we describe the application of this strategy to group 4 metal $(pyCAr_2O)_2M(NMe_2)_2$ complexes. The specific objectives of this study were to develop efficient synthetic routes to $(pyCAr_2O)_2M(NR_2)_2$ complexes and to determine the structures and configurational stability of these species. Initial efforts to activate these compounds for olefin polymerization are also described.

Results

Ligand Synthesis. Pyridine−alcohols **1a**−**g** were prepared by addition of 2-lithiopyridine to the appropriate ketone, followed by aqueous workup, using the approach developed by Holm for **1a** (eq 1).[4] These

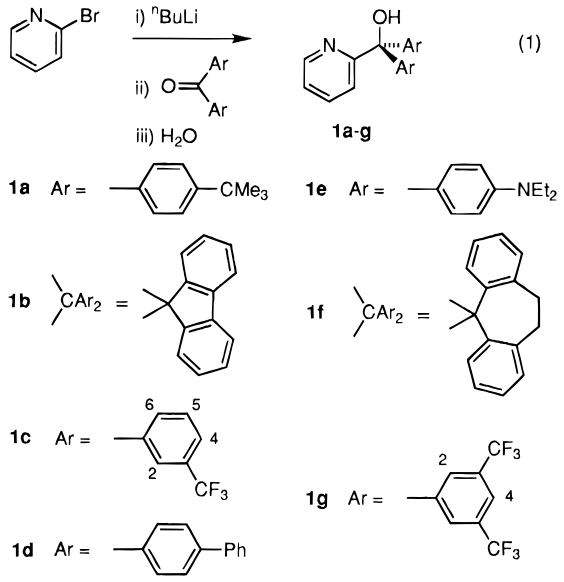

compounds are isolated as sharp-melting white to tan crystalline solids following recrystallization. The use of symmetric ketones yields symmetric $pyCR_2OH$ alcohols, which in turn simplifies the stereochemical possibilities for metal complexes.[1b]

Amine Elimination Reactions. The reactions of $Ti(NMe_2)_4$ with 2 equiv of **1a**−**g** proceed rapidly at room temperature in toluene or benzene to afford NMe_2H and bis(ligand) complexes $(pyCAr_2O)_2Ti(NMe_2)_2$ **2a**−**g** in high yield (eq 2). Complexes **2** were isolated as analytically pure crystalline solids by crystallization from CH_2Cl_2/toluene, except for the fluorinated derivative **2c** which was obtained as an oil. The characterization of these compounds is discussed below.

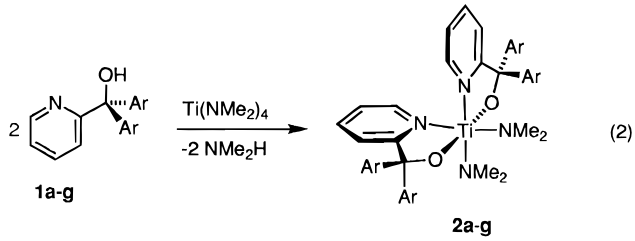

Similarly, the reactions of $Zr(NMe_2)_4$ with 2 equiv of **1a**,**b**,**e** in toluene or benzene produce $(pyCAr_2O)_2Zr(NMe_2)_2$ complexes **3a**,**b**,**e** which are isolated as yellow crystalline solids in high yields (eq 3). However, the

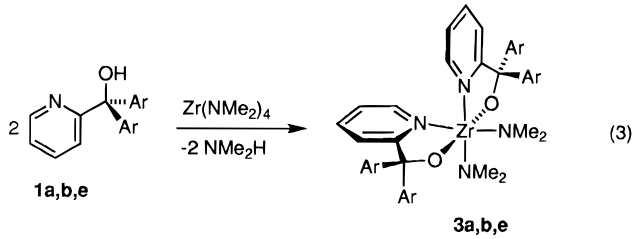

reaction of $Zr(NMe_2)_4$ with the more acidic pyridine alcohol **1c** in benzene or methylene chloride yields a mixture of species assigned as $(pyCAr_2O)_xZr(NMe_2)_{4-x}$ ($x = 1-3$) on the basis of ^1H NMR data. The reaction of $Zr(NMe_2)_4$ with 2 equiv of **1d** yields a similar mixture of products. The tris(ligand) species $(pyCAr_2O)_3Zr(NMe_2)$ (**4c**) was prepared cleanly by reaction of $Zr(NMe_2)_4$ with 3 equiv of **1c** (eq 4). A tetrakis(ligand)

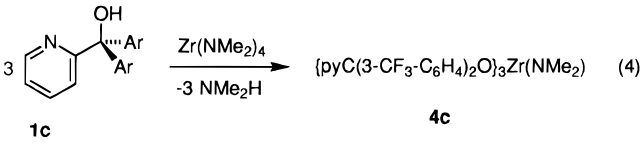

complex $(pyCAr_2O)_4Zr$ (**5e**) was prepared by the reaction of $Zr(NMe_2)_4$ with 4 equiv of **1e** (eq 5), but this species was not studied extensively.

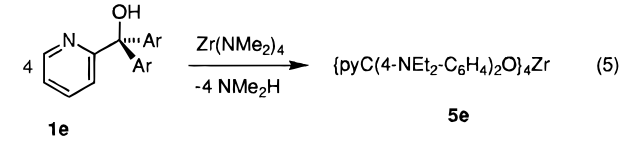

The reactivity of $Hf(NMe_2)_4$ with pyridine−alcohols **1** parallels that of $Zr(NMe_2)_4$. The reaction of $Hf(NMe_2)_4$ with 2 equiv of **1a** or **1e** in toluene or benzene yields the bis(ligand) complexes $(pyCAr_2O)_2Hf(NMe_2)_2$ **6a**,**e** cleanly (eq 6), while reactions with 2 equiv of **1b** or **1c** yield mixtures of products. The tris(ligand) species

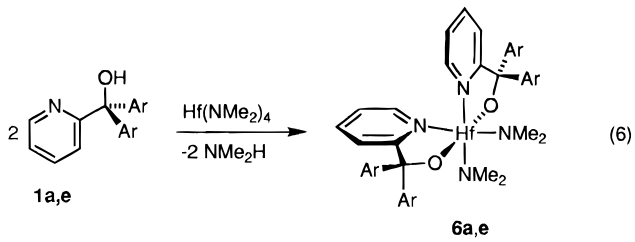

$(pyCAr_2O)_3Hf(NMe_2)$ **7b**,**c** were prepared by reaction of

(2) (a) Diamond, G. M.; Rodewald, S.; Jordan, R. F. *Organometallics* **1995**, *14*, 5. (b) Diamond, G. M.; Jordan, R. F.; Petersen, J. L. *J. Am. Chem. Soc.* **1996**, *118*, 8024. (c) Diamond, G. M.; Jordan, R. F.; Petersen, J. L. *Organometallics* **1996**, *15*, 4030. (d) Christopher, J. N.; Diamond, G. M.; Jordan, R. F.; Petersen, J. L. *Organometallics* **1996**, *15*, 4038. (e) Diamond, G. M.; Jordan, R. F.; Petersen, J. L. *Organometallics* **1996**, *15*, 4045. (f) Christopher, J. N.; Jordan, R. F.; Petersen, J. L.; Young, V. G., Jr. *Organometallics* **1997**, *16*, 3044.

(3) Kim, I.; Jordan, R. F. *Macromolecules* **1996**, *29*, 489.

(4) Schultz, B. E.; Gheller, S. F.; Muetterties, M. C.; Scott, M. J.; Holm, R. H. *J. Am. Chem. Soc.* **1993**, *115*, 2714.

Chart 2

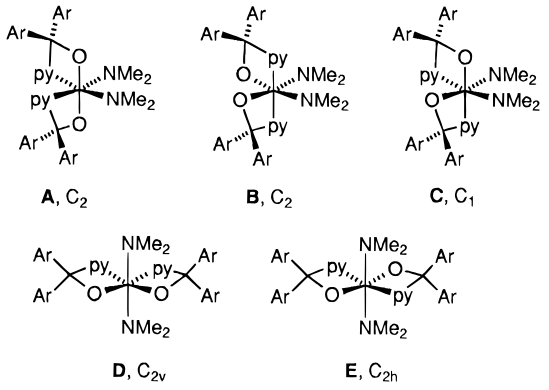

$Hf(NMe_2)_4$ with 3 equiv of **1b**,**c** (eq 7). Complexes **6a**,**e**

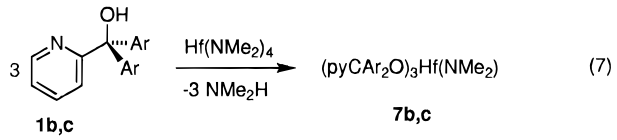

and **7b**,**c** were isolated as yellow solids.

Isolated $(pyCAr_2O)_xM(NMe_2)_{4-x}$ ($x = 2,3$) complexes appear to be stable toward ligand redistribution in CH_2Cl_2 or aromatic solvents at ambient temperature. Thus, the formation of product mixtures in some of the reactions described above results from comparable rates of reaction of the pyridine−alcohols **1** with $(pyCAr_2O)_2M(NMe_2)_2$, $M(NMe_2)_4$, and/or $(pyCAr_2O)M(NMe_2)_3$. In general, less selectivity for the desired $(pyCAr_2O)_2M(NMe_2)_2$ species is observed in reactions of $Zr(NMe_2)_4$ and $Hf(NMe_2)_4$ with the more acidic pyridine−alcohols.

Structural Possibilities for $(pyCAr_2O)_2M(NMe_2)_2$ Complexes. Five idealized octahedral structures are possible for $(pyCAr_2O)_2M(NMe_2)_2$ complexes, **A**−**E** (Chart 2). In the C_2-symmetric structure **A**, the two pyridine−alkoxide ligands and the two amide ligands are equivalent but the two Ar groups on each pyridine−alkoxide ligand are inequivalent. This structure is expected to be favored because the short M−O bonds are *trans* to each other, the strong *trans*-influence amide groups are *trans* to the weak donor pyridine ligands, and the alkoxide oxygens can participate in O−M π-bonding with different metal d orbitals.[1,5] The symmetry properties of **B** are identical to those of **A**; however, **B** should be disfavored by the *cis* orientation of the short M−O bonds and because the alkoxides must share a single metal d orbital for O−M π-donation. Structure **C** is of lower symmetry and contains two inequivalent pyridine−alkoxide and amide ligands; in this case, all four Ar groups are inequivalent. Structures **D** and **E** are of higher symmetry, and in each case, the four Ar groups are equivalent. Isomers **D** and **E** should be disfavored by the *trans* arrangement of the amide ligands, and **E** is also disfavored because only a single metal d orbital can participate in O−M π-bonding in this structure.

Solid State Structures of 2b, 2e, and 3a. As a variety of isomers are possible for $(pyCAr_2O)_2M(NMe_2)_2$ complexes, X-ray crystallographic analyses of representative examples were performed to probe for general structural trends and to determine the bonding properties of $pyCAr_2O^-$ ligands in early metal systems. The molecular structures of **2b**, **2e**, and **3a** are shown in Figures 1−3, and crystallographic data and key metrical parameters are summarized in Tables 1 and 2. All three complexes adopt a distorted octahedral structure of type **A**, with a *trans*-alkoxide, *cis*-pyridine, *cis*-amide ligand arrangement. In these approximately C_2-symmetric structures, one aryl group on each $pyCAr_2O^-$ ligand points over (under) an amide ligand. The distortions from idealized octahedral geometry arise from the acute bite angle of the bidentate $pyCAr_2O^-$ ligands. This bite angle is ca. 73° in **2b** and **2e** and 68° in **3a**.

The structures of titanium complexes **2b** and **2e** are very similar; minor differences in bond angles are observed, which can be traced to the fact that the Ar substituents in **2b** are tied back in the fluorene ring system. The Ar−C−Ar angles in **2b** (C(7)−C(6)−C(18), 101.9(8)°; C(25)−C(24)−C(36), 100.7(8)°) are 10° smaller

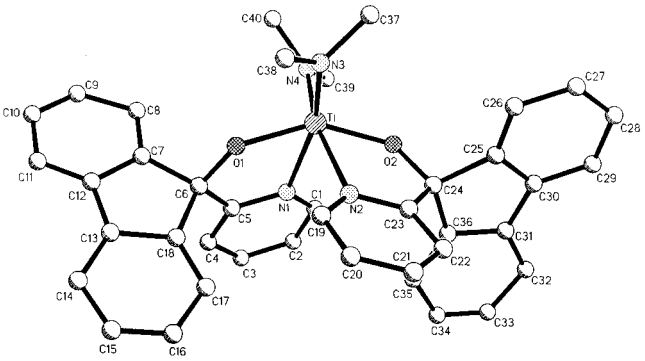

Figure 1. Molecular structure of {9-(2-pyridyl)-9-fluorenolato}$_2$Ti$(NMe_2)_2$ (**2b**).

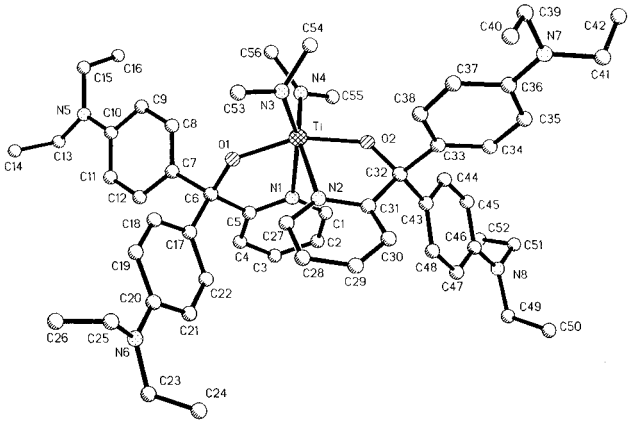

Figure 2. Molecular structure of {pyC(4-NEt_2−C_6H_4)$_2$O}$_2$-Ti$(NMe_2)_2$ (**2e**).

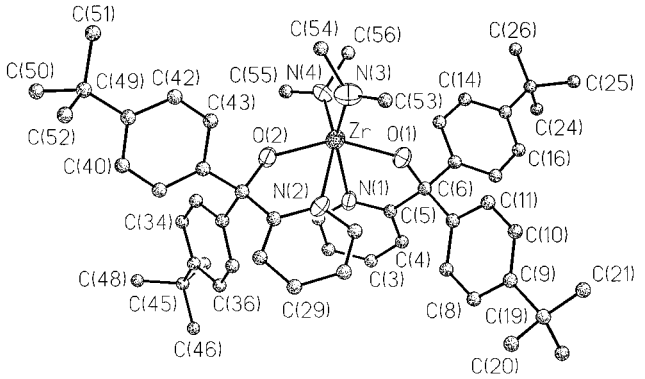

Figure 3. Molecular structure of {pyC(4-^{t}Bu−C_6H_4)$_2$O}$_2$-Zr$(NMe_2)_2$ (**3a**).

(5) Kepert, D. L. In *Progress in Inorganic Chemistry*; Lippard, S. L., Ed.; John Wiley & Sons: New York, 1977; Vol. 23, Chapter 1.

Table 1. Summary of Crystallographic Data

compound	**2b**	**2e**·toluene	**3a**·0.5NMe$_2$H
empirical formula	$C_{40}H_{36}N_4O_2Ti$	$C_{56}H_{76}N_8O_2Ti\cdot C_7H_8$	$C_{56}H_{72}N_4O_2Zr\cdot 0.5NMe_2H$
fw	652.63	1033.28	966.81
cryst size (mm)	0.10 × 0.10 × 0.40	0.15 × 0.30 × 0.40	0.3 × 0.3 × 0.3
color/shape	orange/plate	orange/fragment	colorless/fragment
space group	*Pna*2$_1$	*P*2$_1$/*n*	*P*2$_1$/*n*
a (Å)	17.6747(4)	13.4825(2)	13.095(5)
b (Å)	22.5590(6)	17.9211(3)	17.087(7)
c (Å)	11.3732(2)	27.4775(1)	26.860(10)
β (deg)		97.791(1)	90.95(3)
V (Å^3)	4534.8(2)	6099.08(14)	6010(4)
Z	4	4	4
temp (K)	293	293	296
diffractometer	Siemens SMART, CCD	Siemens SMART, CCD	Siemens P4
radiation, *λ*	Mo Kα, 0.710 73 Å	Mo Kα, 0.710 73 Å	Mo Kα, 0.710 73 Å
monochromator	graphite	graphite	graphite
2*θ* range (deg)	2.92 < 2*θ* < 46.70	2.78 < 2*θ* < 46.70	4.0 < 2*θ* < 45.0
data collected *h*, *k*, *l*	−13 to 19, −25 to 25, −12 to 12	−13 to 15, −19 to 10, −28 to 28	−14 to 14, +18, +28
total no. of reflns collected	17 298	23 505	7944
no. of unique reflns	6165	8697	7760
R_{int}	0.0606	0.0476	
no. of obs reflns, criterion	4598, $I > 2\sigma(I)$	6259, $I > 2\sigma(I)$	3122, $F > 5\sigma(F)$
μ, cm^{-1}	2.19	1.87	2.21
abs corr factors (min/max)	1.051/1.436		
abs corr method	*ψ* scans	none applied	none applied
structure soln	direct methods	direct methods	direct methods
refinement	FMLS on F^2;[a] non-H anisotropic; H calculated	FMLS on F^2;[a] non-H anisotropic; H calculated	FMLS on *F*;[d] N,O,Zr anisotropic; C isotropic; H calculated
R1 ($I > 2\sigma(I)$)	0.1274[b]	0.0707[b]	R(F) = 0.0909[e]
wR2 ($I > 2\sigma(I)$)	0.3162[c]	0.1863[c]	R(wF) = 0.1249[e]
max resid density (e/Å^3)	1.28	0.661	0.65

[a] *SHELXTL*, ver 5; Siemens Analytical X-ray Instruments, Inc.: Madison, WI. [b] $R1 = \sum(|F_o| - |F_c|)/\sum F_o$. [c] $wR2 = \{[\sum w(F_o^2 - F_c^2)^2]/[\sum w(F_o^2)^2]\}^{1/2}$. [d] SHELXTL PLUS (4.2); Siemens Analytical X-Ray Instruments, Inc.: Madison, WI. [e] $F > 5\sigma(F)$; $R(F) = \sum\Delta/\sum F_o$; $R(wF) = \sum\Delta w^{1/2}/\sum(F_o w^{1/2})$; $\Delta = |(F_o - F_c)|$.

Table 2. Selected Bond Distances (Å) and Angles (deg) for 2b, 2e, and 3a

	2b	**2e**	**3a**
M−O(1)	1.909(6)	1.906(2)	2.027(8)
M−O(2)	1.917(6)	1.908(2)	2.038(9)
M−N(1)	2.312(7)	2.313(3)	2.452(11)
M−N(2)	2.315(8)	2.282(3)	2.415(11)
M−N(3)	1.915(8)	1.930(3)	2.055(14)
M−N(4)	1.933(8)	1.932(3)	2.089(13)
O(1)−M−O(2)	149.8(3)	157.25(10)	150.6(4)
N(1)−M−N(3)	165.2(3)	161.36(13)	157.3(5)
N(2)−M−N(4)	167.2(3)	162.31(13)	157.3(4)
O(1)−M−N(1)	73.5(3)	72.39(10)	68.4(4)
O(1)−M−N(2)	86.1(3)	89.20(10)	88.9(4)
O(1)−M−N(3)	91.8(3)	89.23(12)	90.1(5)
O(1)−M−N(4)	106.5(3)	105.16(13)	109.8(4)
O(2)−M−N(1)	86.0(3)	91.34(10)	89.4(4)
O(2)−M−N(2)	73.2(3)	72.97(10)	68.0(4)
O(2)−M−N(3)	108.1(3)	105.37(13)	107.9(5)
O(2)−M−N(4)	94.2(3)	90.43(13)	89.9(4)
N(1)−M−N(2)	93.7(3)	83.88(10)	80.9(4)
N(2)−M−N(3)	86.4(3)	93.03(12)	91.8(5)
N(3)−M−N(4)	95.6(4)	97.4(2)	100.7(5)
N(1)−M−N(4)	87.6(3)	90.60(13)	93.8(4)
M−O(1)−C	128.7(5)	131.0(2)	132.0(8)
M−O(2)−C	128.3(6)	130.0(2)	132.2(8)

than the corresponding angles in **2e** (C(7)−C(6)−C(17), 111.4(3)°; C(33)−C(32)−C(43) 110.9(3)°). In **2e**, the Ar groups can rotate freely to minimize interchelate Ar−py steric interactions, which allows tightening of the N(1)−Ti−N(2) angle by 10° relative to that in **2b**. For both structures, the O(1)−Ti−N(3) and O(2)−Ti−N(4) angles are very close to 90° and the N(3)−Ti−N(4) angles are ca. 96°.

The Ti−O−C units in **2b** and **2e** are bent (Ti−O−C ca. 130°), and the oxygens are, therefore, sp^2-hybridized and have only one p orbital available for O−Ti *π*-bonding. The amide nitrogens are flat and also have one p orbital available for N−Ti *π*-bonding. Thus, in these six-coordinate complexes, the four ligand *π*-donor orbitals compete for *π*-bonding with three metal d acceptor orbitals and partial Ti−O and Ti−N$_{amide}$ *π*-bonding is expected. Consistent with this analysis, the Ti−O distances in **2b** and **2e** (average 1.910(4) Å) are shorter than the Ti−O *σ*-bond distance predicted on the basis of covalent radii (ca. 1.99−2.05 Å)[6] but longer than Ti−O distances observed in more highly electron-deficient Ti(IV) alkoxides; e.g., TiCl$_2$(O-2,6-Ph$_2$−C$_6$H$_3$)$_2$ (1.73 Å),[7] [TiCl$_2$(OPh)]$_2$(*μ*-OPh)$_2$ (terminal Ti−O 1.75 Å),[8] Ti{*O*-2-^{t}Bu−C$_6$H$_4$}$_4$ (1.78 Å),[9] and [Ti(CH$_2$Ph)$_2$(OEt)]$_2$(*μ*-OEt)$_2$ (terminal Ti−O 1.84 Å).[10] Similarly, the Ti−N$_{amide}$ distances in **2b** and **2e** (average 1.928(7) Å) are shorter than the predicted Ti−N *σ*-bond distance (ca. 2.02−2.07 Å)[6] but longer than those observed for four-coordinate Ti(IV) amides; e.g., Ti{*O*-2,4,6-(^{t}Bu)$_3$−C$_6$H$_2$}$_2$(NMe$_2$)$_2$ (average 1.88 Å),[11] CpFe(CO)$_2$Ti(NMe$_2$)$_3$ (average 1.88 Å),[12] and Ti(O-2,6-Ph$_2$−C$_6$H$_3$)$_2$(NHPh)$_2$ (average 1.88 Å).[13,14]

The pyridine−alkoxide chelate rings in **2b** and **2e** are flat and do not appear to be significantly strained. However, inspection of the angles around the pyridine

(6) Ranges for Ti−O and Ti−N *σ* bond distances were estimated using covalent radii taken from the following: (a) Porterfield, W. M. *Inorganic Chemistry*; Academic Press: San Diego, CA, 1993; p 214 (Ti, 1.32 Å; O, 0.73 Å, N, 0.75 Å). (b) Jolly, W. L. *Modern Inorganic Chemistry*; McGraw-Hill, Inc.: New York, 1984, p 52 (O, 0.66 Å; N, 0.70 Å).

(7) Dilworth, J. R.; Hanich, J.; Krestel, M.; Beck, J.; Strahle, J. *J. Organomet. Chem.* **1986**, *315*, C9.
(8) Watenpaugh, K.; Caughlan, C. N. *Inorg. Chem.* **1966**, *5*, 1782.
(9) Toth, R. T.; Stephan, D. W. *Can. J. Chem.* **1991**, *69*, 172.
(10) Stoeckli-Evans, H. *Helv. Chim. Acta.* **1975**, *58*, 373.
(11) Jones, R. A.; Hefner, J. G.; Wright, T. C. *Polyhedron* **1984**, *3*, 1121.
(12) Sartain, W. J.; Selegue, J. P. *Organometallics* **1987**, *6*, 1812.
(13) Zambrano, C. H.; Profilet, R. D.; Hill, J. E.; Fanwick, P. E.; Rothwell, I. P. *Polyhedron* **1993**, *12*, 689.

nitrogen reveals that the metal atom is displaced 5−8° (toward the oxygen) off of the axis which would maximize py−Ti bonding. For example in **2b**, the Ti−N(2)−C(19) angle (128.2(7)°) is significantly larger than the Ti−N(2)−C(23) angle (112.6(6)°).

The structure of zirconium complex **3a** is very similar to those of **2b** and **2e**. The minor differences in bond angles result from the longer M−L bond lengths. The structures of all three complexes are closely comparable to those of other group 4 metal $(N,O$-chelate$)_2MX_2$ compounds containing bidentate N,O-chelate ligands which form five-membered chelate rings, including $(Ox)_2TiCl_2$,[15] $(Ox)_2Ti\{O$-2,6-$(^iPr)_2-C_6H_3\}_2$, $(MeOx)_2Ti\{O$-2,6-$(^iPr)_2-C_6H_3\}_2$,[16] $(MeOx)_2Zr(CH_2Ph)_2$,[1a] and $(pyCMe_2O)_2Zr(CH_2Ph)_2$.[1b]

Solution Structures and Dynamic Properties of $(pyCAr_2O)_2M(NMe_2)_2$ Complexes. As summarized in the experimental section, the ambient-temperature ^1H NMR spectra of $(pyCAr_2O)_2M(NMe_2)_2$ complexes each contain a singlet for the NMe_2 groups, a single set of four multiplets for the four pyridine hydrogens, and single set of resonances for the Ar group; in most cases, the aromatic resonances for the Ar groups are broad. The ambient-temperature ^{13}C NMR spectra are analogous and contain a single NMe_2 resonance, a single set of pyridine resonances, and a single set of Ar resonances which are broadened in some cases. To probe the fluxional behavior implied by the broadened Ar resonances and to establish static structures, low-temperature ^1H NMR spectra of representative complexes were investigated.

The $\{pyC(4\text{-}^tBu-C_6H_4)_2O\}_2M(NMe_2)_2$ complexes **2a**, **3a**, and **6a** were investigated initially because it was anticipated that the ^{t}Bu resonance would serve as a sensitive reporter of the Ar group environments. For hafnium complex **6a**, the sharp pyridine and NMe_2 resonances do not change when the temperature is lowered to −40 °C. However, the aromatic resonances for the Ar groups, which comprise a doublet and a broad singlet at ambient temperature, sharpen to three doublets (2/1/1 intensity ratio) as the temperature is lowered. Additionally, the sharp ^{t}Bu resonance splits to two singlets (1/1 intensity ratio). The variable-temperature NMR behavior of **2a** and **3a** is analogous.[17] These observations establish that the static structures of **2a**, **3a**, and **6a** contain two equivalent pyridine groups, two equivalent NMe_2 groups, and two inequivalent sets of two Ar groups, i.e., the static structures are of type **A** or **B** (Chart 2). On the basis of the solid state structures of **2b**, **2e**, and **3a**, we conclude that **2a**, **3a**, and **6a** adopt structures of type **A** in CD_2Cl_2 solution. However, these complexes undergo rapid inversion of metal configuration which renders the four Ar groups equivalent. Racemization barriers calculated from the coalescence of the ^{t}Bu resonances are listed in Table 3.[18]

Table 3. Racemization Barriers for $(pyCAr_2O)_2M(NMe_2)_2$ Complexes

complex	$\Delta G^‡$ (racemization) (kcal/mol)
$\{pyC(4\text{-}^tBu-C_6H_4)_2O\}_2Ti(NMe_2)_2$ (**2a**)	13.1(2)
$\{pyC(3\text{-}CF_3-C_6H_4)_2O\}_2Ti(NMe_2)_2$ (**2c**)	12.6(3)
{11-(2-pyridyl)dibenzosuberolato}$_2$Ti$(NMe_2)_2$ (**2f**)	12.2(2)
$\{pyC(3,5\text{-}(CF_3)_2-C_6H_3)_2O\}_2Ti(NMe_2)_2$ (**2g**)	12.5(2)
$\{pyC(4\text{-}^tBu-C_6H_4)_2O\}_2Zr(NMe_2)_2$ (**3a**)	12.2(2)
$\{pyC(4\text{-}^tBu-C_6H_4)_2O\}_2Hf(NMe_2)_2$ (**6a**)	13.2(2)
$\{pyC(4\text{-}NEt_2-C_6H_4)_2O\}_2Hf(NMe_2)_2$ (**6e**)	14.0(1)

The ^1H NMR spectrum of $\{pyC(3\text{-}CF_3-C_6H_4)_2O\}_2Ti(NMe_2)_2$ (**2c**) at 0 °C contains a single set of sharp pyridine resonances, a singlet for the NMe_2 groups, and broad resonances for the Ar hydrogens. As the temperature is lowered, the pyridine and NMe_2 resonances remain essentially unchanged but the Ar region sharpens to a complex pattern which is consistent with the presence of two Ar environments. In particular, two broad singlets (1/1 intensity ratio) for the H2 hydrogens (see numbering scheme in eq 1) appear at −20 °C and sharpen as the temperature is lowered further. These observations are consistent with a static structure of type **A** for **2c** and rapid racemization at ambient temperature. The racemization barrier was determined from the line broadening of the H2 resonances (Table 3).[19] Similar dynamic NMR behavior is observed for **2f**, **2g**, and **6e**, indicating that these species adopt C_2-symmetric structures and undergo rapid inversion of metal configuration at ambient temperature.[20−22]

On the basis of the X-ray structural and low-temperature NMR results for representative compounds discussed above and the similarity of the ambient-temperature NMR data for all of the compounds studied (in particular the presence of sharp pyridine and NMe_2 resonances and broad aromatic Ar resonances), we conclude that group 4 metal $(pyCAr_2O)_2M(NMe_2)_2$ complexes adopt type **A** structures in general but undergo facile racemization which is rapid on the NMR time scale at room temperature.

The free energy barriers for racemization of $(pyCAr_2O)_2M(NMe_2)_2$ complexes (Table 3) are insensitive to the ligand structure and the identity of the metal. The $\Delta G^‡$ (racemization) values for the titanium complexes vary by less than 1 kcal/mol, despite the significant variation in ligand electronic properties (e.g., **2a** vs **2g**) and rigidity (**2f** vs **2a**,**c**,**g**). The $\Delta G^‡$ (racemization) values for analogous Ti, Zr, and Hf complexes **2a**, **3a**, and **6a** also vary by less than 1 kcal/mol. Previous work by Bickley and Serpone shows that $(Ox)_2Ti\{O$-2,6-$(^iPr)_2-C_6H_3\}_2$ and $(MeOx)_2Ti\{O$-2,6-$(^iPr)_2-C_6H_3\}_2$ undergo inversion of metal configuration via five-coordinate trigonal bipyramidal intermediates formed by

(14) The ionic character of the M−O and M−N_{amide} bonds in $(pyCAr_2O)_2M(NR_2)_2$ species also contributes to the shortening of the bond distances from the values predicted on the basis of covalent radii. For a discussion and listing of key references regarding this point, see: Howard, W. A.; Trnka, T. M.; Parkin, G. *Inorg. Chem.* **1995**, *34*, 5900.

(15) Studd, B. F.; Swallow, A. G. *J. Chem. Soc. A* **1968**, 1961.

(16) Bird, P. H.; Fraser, A. R.; Lau, C. F. *Inorg. Chem.* **1973**, *12*, 1322.

(17) Coalescence of ^{t}Bu resonances. For **2a**: $T_c = 268$ K, $\Delta\nu = 52$ Hz; $\Delta G^‡ = 13.1(2)$ kcal/mol. For **3a**: $T_c = 248$ K, $\Delta\nu = 43$ Hz; $\Delta G^‡ = 12.2(2)$ kcal/mol. For **6a**: $T_c = 268$ K, $\Delta\nu = 43$ Hz; $\Delta G^‡ = 13.2(2)$ kcal/mol.

(18) The barriers estimated from changes in the aromatic region are similar but were less precisely determined due to overlapping resonances which precluded accurate determination of coalescence temperatures.

(19) For **2c**: $w_{1/2}$(excess) for the H2 resonances = 20 Hz at 253K, corresponding to $k_{exchange} = 63$ s^{-1} and $\Delta G^‡ = 12.6(3)$ kcal/mol. The coalescence point could not be determined due to interference from the other Ar and py resonances.

(20) For **2f**: Coalescence of δ 6.03 and 5.87 doublets, $T_c = 250$ K, $\Delta\nu = 54$ Hz; $\Delta G^‡ = 12.2(2)$ kcal/mol.

(21) For **2g**: Coalescence of the Ar H2 signals (δ 8.02, 7.42), $T_c = 273$ K, $\Delta\nu = 214$ Hz, $\Delta G^‡ = 12.5(2)$ kcal/mol; coalescence of Ar H4 signals (δ 7.94, 7.83), $T_c = 254$ K, $\Delta\nu = 42$ Hz, $\Delta G^‡ = 12.5(2)$ kcal/mol.

(22) For **6e**: Coalescence of δ 7.16 and 6.80 doublets, $T_c = 298$ K, $\Delta\nu = 335$ Hz; $\Delta G^‡ = 14.0(1)$ kcal/mol.

Table 4. Ethylene Polymerization Results[a]

run	catalyst	μmol of catalyst	cocatalysts[b]	time (h)	yield (g)	activity (kg/(mol·atm·h))	M_w ($\times 10^{-3}$)	M_w/M_n	T_m[c]
1	{pyC(4-^{t}Bu−Ph)$_2$O}$_2$Ti(NMe$_2$)$_2$ (**2a**)	6.8	Al(^{i}Bu)$_3$ + MAO	1	0.17	25	122	24.1	128.9
2	{pyC(4-^{t}Bu−Ph)$_2$O}$_2$Zr(NMe$_2$)$_2$ (**3a**)	5.4	Al(^{i}Bu)$_3$ + MAO	1	1.5	280	88	8.3	132.5
3	{pyC(4-NEt$_2$−Ph)$_2$O}$_2$Ti(NMe$_2$)$_2$ (**2e**)	5.3	Al(^{i}Bu)$_3$ + MAO	2	0.77	73			
4	{pyC(4-NEt$_2$−Ph)$_2$O}$_2$Zr(NMe$_2$)$_2$ (**3e**)	5.1	Al(^{i}Bu)$_3$ + MAO	2	1.3	120			
5	{pyC(4-Ph−Ph)$_2$O}$_2$Ti(NMe$_2$)$_2$ (**2d**)	5.2	Al(^{i}Bu)$_3$ + MAO	1	0.26	49	105	8.7	126.2
6	{9-(2-pyridyl)-9-flu}$_2$Ti(NMe$_2$)$_2$ (**2b**)	7.2	Al(^{i}Bu)$_3$ + MAO	1	0.18	25			

[a] Conditions: toluene (120 mL), 1 atm of ethylene, T = 43 °C. [b] Al(^{i}Bu)$_3$: 4.0 mmol. MAO: 7.0 mmol. Al/M = ca. 2000. [c] DSC peak mp.

pyridine dissociation.[23] A similar "bond rupture" mechanism is likely for the (pyCAr$_2$O)$_2$M(NMe$_2$)$_2$ systems studied here (eq 8). The lack of influence of ligand

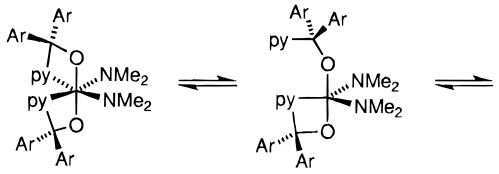

Λ-(pyCAr$_2$O)$_2$M(NMe$_2$)$_2$

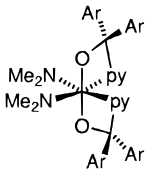

Δ-(pyCAr$_2$O)$_2$M(NMe$_2$)$_2$ (8)

structure or metal identity on the $\Delta G^{\ddagger}$ (racemization) values presumably reflects the fact that (i) the electronic differences between the pyCAr$_2$O$^-$ ligands in these compounds are located at the Ar groups and not the py groups and (ii) steric interactions in these systems are similar. The racemization barriers observed for (pyCAr$_2$O)$_2$M(NMe$_2$)$_2$ compounds (12−14 kcal/mol) are lower than those observed for (Ox)$_2$Ti{*O*-2,6-(^{i}Pr)$_2$−C$_6$H$_3$}$_2$ (20.0(3) kcal/mol), (MeOx)$_2$Ti{*O*-2,6-(^{i}Pr)$_2$−C$_6$H$_3$}$_2$ (17.1(3) kcal/mol), (MeOx)$_2$Zr(CH$_2$CMe$_3$)$_2$ (15.1(1) kcal/mol), (MeBr$_2$Ox)$_2$Zr(CH$_2$CMe$_3$)$_2$ (15.7(1) kcal/mol), and (MeBr$_2$Ox)$_2$Hf(CH$_2$Ph)$_2$ (17.5(1) kcal/mol).[1a,23] This difference presumably results from the increased flexibility of the pyCAr$_2$O$^-$ ligands versus the quinolinolato ligands. On the other hand, much lower barriers (ca. 8−10 kcal/mol) were observed for (pyCR$_2$O)$_2$M(CH$_2$Ph)$_2$ complexes (R = CF$_3$, Me, H; M = Ti, Zr) which contain alkyl substituents at the alkoxide carbon of the pyCR$_2$O$^-$ ligands.[1b,c]

The ambient-temperature ^{1}H and ^{13}C NMR spectra of tris(ligand) (pyCAr$_2$O)$_3$M(NMe$_2$) complexes **4c**, **7b**, and **7c** exhibit a single set of pyCAr$_2$O$^-$ ligand resonances. In each case, the pyridine *ortho*-hydrogen ^{1}H resonance appears as a broad singlet downfield from the position observed for the corresponding resonance in (pyCAr$_2$O)$_2$M(NMe$_2$)$_2$ complexes and in the range observed for the free pyridine−alcohols. The ^{1}H NMR spectrum of **4c** becomes more complex when the temperature is lowered; however, a limiting spectrum was not reached at −80 °C and a static structure could not be established. Thus, these (pyCAr$_2$O)$_3$M(NMe$_2$) species are highly fluxional and may adopt structures with at least one uncoordinated pyridine group. The tetrakis(ligand) complex **5e** is also highly fluxional, and low-temperature NMR data (to −80 °C) do not allow structural assignment in this case.[24]

Olefin Polymerization Studies. The ethylene polymerization behavior of several (pyCAr$_2$O)$_2$M(NMe$_2$)$_2$ and (pyCAr$_2$O)$_3$M(NMe$_2$) complexes has been investigated using the *in situ* alkylation/activation protocol developed earlier for ^{ch}Cp$_2$Zr(NMe$_2$)$_2$ metallocene amide compounds.[3] The metal amide complex was treated with excess Al(^{i}Bu)$_3$ in toluene, activated with MAO, and charged with ethylene (1 atm). The working hypothesis of these experiments was that the AlR$_3$ reagent and activator would generate (pyCAr$_2$O)$_2$M(R)$^+$ or (pyCAr$_2$O)$_2$M(H)$^+$ species *in situ*, by analogy to the results observed in analogous experiments with ^{ch}Cp$_2$Zr(NMe$_2$)$_2$ complexes. The results are summarized in Table 4. The *in situ* alkylation/activation procedure activates (pyCAr$_2$O)$_2$Ti(NMe$_2$)$_2$ and (pyCAr$_2$O)$_2$Zr(NMe$_2$)$_2$ complexes for ethylene polymerization but not the corresponding Hf compounds. The catalysts derived from (pyCAr$_2$O)$_2$Zr(NMe$_2$)$_2$ species are more active than the corresponding Ti catalysts (run 1 vs 2; run 3 vs 4) under the conditions studied (toluene, 43 °C, 1 atm). However, no clear ligand effects on activity are evident from the limited data yet available.

The catalysts derived from (pyCAr$_2$O)$_2$M(NMe$_2$)$_2$ (M = Ti, Zr) produce linear polyethylene (by ^{13}C NMR) with a very broad molecular weight distribution; in most cases, the distributions are multimodal, characteristic of multisite catalysts. Thus, the catalyst activation chemistry is more complex than that observed for ^{ch}Cp$_2$Zr(NMe)$_2$ catalysts. Earlier, we showed that ^{ch}Cp$_2$Zr(NMe)$_2$ complexes are cleanly converted to ^{ch}Cp$_2$ZrR$_2$ complexes upon reaction with AlR$_3$ reagents.[2,3] However, (Ox)$_2$M(NMe$_2$)$_2$ and (pyCR$_2$O)$_2$MR$_2$ complexes react with AlMe$_3$ via Ox$^-$ or pyCR$_2$O$^-$ transfer yielding (Ox)AlMe$_2$ or (pyCR$_2$O)AlMe$_2$ as the principal products.[1] It is likely the reaction of (pyCAr$_2$O)$_2$M(NMe$_2$)$_2$ complexes with Al(^{i}Bu)$_3$ or MAO can result in transfer of either a Me$_2$N$^-$ or a pyCAr$_2$O$^-$ ligand to Al, ultimately generating several metal alkyl species which are active for ethylene polymerization. This issue is under investigation.

Further investigations of these catalysts and parallel studies of (pyCAr$_2$O)$_2$M(R)$^+$ cations are in progress.[1c]

Summary. Amine elimination reactions of pyCAr$_2$OH pyridine−alcohols and group 4 metal M(NMe$_2$)$_4$ amides provide an efficient entry to (pyCAr$_2$O)$_2$M(NMe$_2$)$_2$ complexes. These species adopt C_2-symmetric structures in the solid state and in solution but undergo facile inversion of configuration at the metal, with

(23) Bickley, D. G.; Serpone, N. *Inorg. Chem.* **1979**, *8*, 2200.

(24) The structure of (Ox)$_4$Zr has been determined by X-ray crystallography, see: Lewis, D. F.; Fay, R. C. *J. Chem. Soc., Chem. Commun.* **1974**, 1046.

racemization barriers in the range of 12−14 kcal/mol. The racemization barriers are insensitive to the Ar group structure or the metal (Ti, Zr, Hf). These amide complexes are activated for ethylene polymerization by alkylation with AlR_3 reagents and subsequent reaction with MAO; however, the molecular weight distributions of the polymer products are broad and show multimodal character characteristic of multisite catalysts. The reaction of the more acidic $pyCAr_2OH$ alcohols **1c** or **1d** with $Zr(NMe_2)_4$ and the reactions of **1b**, **1c** or **1d** with $Hf(NMe_2)_4$ yield mixtures of $(pyCAr_2O)_xM(NMe_2)_{4-x}$ ($x = 1-3$) species. The $\{pyCAr_2O\}_3M(NMe_2)$ tris(ligand) species **4c** and **7b**,**c** can be obtained by suitable adjustment of the reaction stoichiometry.

Experimental Section

General Procedures. All experiments were performed on a high-vacuum line or in a drybox under a purified N_2 atmosphere. NMR spectra were recorded on a Bruker AC-300 or AMX-360 spectrometer in sealed or Teflon-valved tubes at ambient probe temperature unless otherwise indicated. ^1H and ^{13}C chemical shifts are reported versus $SiMe_4$ and were determined by reference to the residual solvent peaks. Elemental analyses were performed by E & R Microanalytical Laboratory, Inc., or Desert Analytics. Solvents were dried over Na/benzophenone ketyl, except for chlorinated solvents, which were distilled from activated molecular sieves (3 Å) or P_2O_5. 2-Bromopyridine was distilled from CaH_2 prior to use. The ketones 3,3′-bis(trifluoromethyl)benzophenone, 9-fluorenone, 4,4′-diphenylbenzophenone, 4,4′-bis(dimethylamino)benzophenone, 3,3′,5,5′-tetrakis(trifluoromethyl)benzophenone, and dibenzosuberone were obtained from Aldrich. The following compounds were prepared by literature procedures: 4,4′-di-*tert*-butylbenzophenone,[25] bis(4-*tert*-butylphenyl)-2-pyridylmethanol (**1a**), $Ti(NMe_2)_4$, $Zr(NMe_2)_4$, and $Hf(NMe_2)_4$.[2,26]

Compounds **2a**, **3a**, and **6a**, which contain $pyC(4\text{-}^tBu-C_6H_4)_2O^-$ ligands, were too soluble for conventional recrystallization. However, these compounds were obtained as analytically pure crystalline solids by careful control of reaction stoichiometry and subsequent slow evaporation of solvent from CH_2Cl_2 solution. Compounds **4c** and **5e** were also found to be extremely soluble and could not be recrystallized but were obtained as analytically pure materials in a similar manner.

9-(2-Pyridyl)-9-fluorenol (1b). A solution of 9-fluorenone (10.2 g, 55.4 mmol) in ether (80 mL) was added dropwise to a solution of 2-lithiopyridine (from 66.5 mmol of 2-bromopyridine and ^{n}BuLi) in ether (100 mL) at −78 °C (dry ice/acetone). The addition was made over 90 min, and the temperature was maintained at −78 °C for a further 3 h. The cold bath was removed, and the dark green viscous reaction mixture was stirred overnight at ambient temperature, hydrolyzed with water, and neutralized. The ether layer was separated and washed with water. The aqueous layer was extracted with ether. The ether layer and ether extract were combined, dried over $MgSO_4$, and evaporated to dryness under vacuum. The off-white solid was recrystallized from ether and then from toluene to afford a white crystalline solid. Yield 12.9 g, 75%; mp 130−131 °C. ^1H NMR (CD_2Cl_2): δ 8.61 (d, J = 3.9 Hz, 1H), 7.74 (d, J = 7.6 Hz, 2H), 7.47 (td, J = 8.8, 1.6 Hz, 1H), 7.41 (td, J = 8.5, 1.9 Hz, 2H), 7.24 (m, 5H), 6.63 (d, J = 8.0 Hz, 1H), 6.43 (s, 1H). $^{13}C\{^1H\}$ NMR (CD_2Cl_2): 161.2, 150.2, 147.7, 140.6, 137.5, 129.4, 128.5, 124.7, 123.1, 120.5, 120.4, 83.0. Anal. Calcd for $C_{18}H_{13}NO$: C, 83.38; H, 5.05; N, 5.40. Found: C, 83.38; H, 5.20; N, 5.41.

Bis(3-(trifluoromethyl)phenyl)-2-pyridylmethanol ($pyC(3\text{-}CF_3-C_6H_4)_2OH$, 1c). A solution of 3,3′-bis(trifluoromethyl)benzophenone (8.00 g, 25.1 mmol) in ether (80 mL) was added dropwise to a solution of 2-lithiopyridine (from 30.0 mmol of 2-bromopyridine and ^{n}BuLi) in ether (100 mL) at −78 °C. The addition was made over 2 h, and the temperature was maintained at −78 °C for an additional 3 h. The cold bath was removed, and the dark green reaction mixture was stirred overnight at ambient temperature, resulting in a viscous brown solution. To this solution was added 50 mL of H_2O containing 5.00 g of $[NH_4]Cl$. The solution was neutralized, and the product was isolated and recrystallized as described above for **1b**. Yield 8.12 g, 68%; white crystals; mp 84−85 °C. ^1H NMR (C_6D_6): δ 8.06 (d, J = 4.8 Hz, 1H), 7.87 (s, 2H), 7.29 (d, J = 7.9 Hz, 2H), 7.24 (d, J = 7.8 Hz, 2H), 6.85 (t, J = 7.8 Hz, 2H), 6.80 (td, J = 7.7, 1.7 Hz, 1H), 6.65 (d, J = 6.9 Hz, 1H), 6.43 (m, 1H), 6.40 (s, 1H). $^{13}C\{^1H\}$ NMR (C_6D_6): 161.8, 148.2, 147.4, 136.7, 132.0, 130.8 (q, J_{CF} = 32 Hz), 129.0, 124.9 (q, J_{CF} = 4 Hz), 124.8 (q, J_{CF} = 273 Hz), 124.7 (q, J_{CF} = 4 Hz), 122.8, 122.4, 80.6. Anal. Calcd for $C_{20}H_{13}F_6NO$: C, 60.46; H, 3.30; N, 3.53. Found: C, 60.62; H, 3.30; N, 3.65.

Bis(4-phenylphenyl)-2-pyridylmethanol ($pyC(4\text{-}Ph-C_6H_4)_2OH$, 1d). A slurry of 4,4′-diphenylbenzophenone (8.00 g, 23.9 mmol) in ether (120 mL) was added in portions to a solution of 2-lithiopyridine (obtained from 26.3 mmol of 2-bromopyridine and ^{n}BuLi) in ether (80 mL) at −78 °C. The addition was made over 2 h, and the temperature was maintained at −78 °C for an additional 3 h. The cold bath was removed, and the dark green reaction mixture was stirred overnight at ambient temperature and then refluxed for 3 h. The product was isolated and recrystallized as described above for **1b**. Yield 7.84 g, 72%; white crystals;, mp 170−172 °C. ^1H NMR (C_6D_6): δ 8.23 (d, J = 4.7 Hz, 1H), 7.60 (d, J = 8.4 Hz, 4H), 7.47 (m, 8H), 7.19 (t, J = 8.0 Hz, 4H), 7.10 (t, J = 7.2 Hz, 2H), 7.02 (d, J = 7.9 Hz, 1H), 6.92 (td, J = 7.6, 1.7 Hz, 1H), 6.62 (s, 1H), 6.52 (m, 1H). $^{13}C\{^1H\}$ NMR (CD_2Cl_2): 163.4, 148.2, 145.7, 141.0, 140.5, 137.0, 129.2, 129.0, 127.7, 127.3, 127.0, 123.2, 123.0, 80.9. Anal. Calcd for $C_{30}H_{23}NO$: C, 87.14; H, 5.61; N, 3.39. Found: C, 87.14; H, 5.56; N, 3.59.

Bis(4-(diethylamino)phenyl)-2-pyridylmethanol ($pyC(4\text{-}NEt_2-C_6H_4)_2OH$, 1e). A solution of 4,4′-bis(diethylamino)benzophenone (8.00 g, 24.7 mmol) in ether (120 mL) was added dropwise at −78 °C to a solution of 2-lithiopyridine (generated from 27.1 mmol of 2-bromopyridine and ^{n}BuLi) in ether (80 mL). The addition was made over 2 h and the reaction temperature was maintained at −78 °C for a further 3 h. The cold bath was removed, and the dark green reaction mixture was stirred overnight at ambient temperature. The product was isolated and recrystallized as described above for **1b**. Yield 8.62 g, 79%; tan crystals; mp 106−107 °C. ^1H NMR (CD_2Cl_2): δ 8.56 (d, J = 4.9 Hz, 1H), 7.64 (td, J = 7.8, 1.8 Hz, 1H), 7.19 (m, 2H), 7.09 (d, J = 9.0 Hz, 4H), 6.61 (d, J = 9.0 Hz, 4H), 5.88 (s, 1H), 3.35 (q, J = 7.0 Hz, 8H), 1.16 (t, J = 7.0 Hz, 12H). $^{13}C\{^1H\}$ NMR (CD_2Cl_2): 165.3, 147.8, 147.1, 136.5, 133.8, 129.4, 123.1, 122.2, 111.1, 80.5, 44.7, 12.7. Anal. Calcd for $C_{26}H_{33}N_3O$: C, 77.38; H, 8.24; N, 10.41. Found: C, 77.24; H, 8.49; N, 10.40.

1-(2-pyridyl)dibenzosuberol (1f). A solution of dibenzosuberone (9.98 mL, 55.4 mmol) in ether (80 mL) was added dropwise over 90 min to a solution of 2-lithiopyridine (from 66.5 mmol of 2-bromopyridine and *n*-BuLi) in ether (100 mL) at −78 °C. The temperature was maintained at −78 °C for a further 3 h. The cold bath was removed, and the dark red reaction mixture was stirred overnight at room temperature. During this period, the color turned to greenish black. Water (50 mL) was added, and the mixture was stirred for 1 h. The ether and water phases were separated, and the water phase was extracted with dichloromethane (4 × 50 mL). The extracts were combined with the ether phase, dried over $MgSO_4$, and evaporated to give a pale yellow solid. Recrystallization from methanol gave a white crystalline solid. Yield 11.0 g, 69%; mp 198−199 °C. ^1H NMR ($CDCl_3$): δ 8.51 (dq, J = 4.0, 0.9

(25) (a) Larner, B.; Peters, A. T. *J. Chem. Soc.* **1952**, 880. (b) Buu-Hoi, N. P.; Royer, R.; Xuong, N. D.; Thang, K. V. *Bull. Soc. Chim. Fr.* **1955**, 1204.

(26) (a) Bradley, D. C.; Thomas, I. M. *Proc. Chem. Soc.* **1959**, 225; *J. Chem. Soc.* **1960**, 3857. (b) Chisholm, M. H.; Hammond, C. E.; Huffman, J. C. *Polyhedron* **1988**, *7*, 2515.

Hz, 1H), 7.99 (dd, J = 7.8, 1.5 Hz, 2H), 7.55 (td, J = 7.7, 1.8 Hz, 1H), 7.26 (td, J = 7.4, 1.6 Hz, 2H), 7.20 (td, J = 7.3, 1.5 Hz, 2H), 7.13 (ddd, J = 8.5, 4.8, 1.0 Hz, 1H), 7.08 (dd, J = 7.3, 1.3 Hz, 2H), 7.05 (dt, J = 7.9, 0.9 Hz, 1H), 3.80 (br s, 1H, −OH), 2.96−2.76 (m, 4H). ^{13}C{^{1}H} NMR ($CDCl_3$): 166.0, 149.4, 142.7, 137.8, 136.5, 130.2, 127.7, 126.2, 125.9, 122.2, 121.8, 80.0, 32.8. Anal. Calcd for $C_{20}H_{17}NO$: C, 83.60; H, 5.96; N, 4.87. Found: C, 83.59; H, 5.81; N, 4.81.

Bis(3,5-bis(trifluoromethyl)phenyl)-2-pyridylmethanol (pyC(3,5-(CF$_3$)$_2$−C$_6$H$_3$)$_2$OH, 1g). A solution of 2-lithiopyridine (from 11.0 mmol of 2-bromopyridine and *n*-BuLi) in ether (20 mL) was added dropwise over 30 min to a solution of 3,3′,5,5′-tetrakis(trifluoromethyl)benzophenone (4.54 g, 10.0 mmol) in ether (30 mL) at −78 °C. The temperature was maintained at −78 °C for a further 3 h. The cold bath was removed, and the dark red reaction mixture was stirred overnight at room temperature. Aqueous [NH_4]Cl (4.6 M, 50 mL) was added. The mixture was extracted with dichloromethane (4 × 25 mL). The extract was dried over $MgSO_4$ and evaporated to give a brown viscous oil. Recrystallization from hexanes gave a colorless crystalline solid. Yield 1.6 g, 30%; mp 74−75 °C. ^{1}H NMR ($CDCl_3$): δ 8.66 (dt, J = 4.8, 1.0 Hz, 1H), 7.84 (s, 2H), 7.78 (td, J = 7.7, 1.7 Hz, 1H), 7.72 (s, 4H), 7.38 (ddd, J = 7.5, 5.7, 0.8 Hz, 1H), 7.06 (d, J = 7.9 Hz, 1H), 6.62 (br s, 1H, OH). ^{13}C{^{1}H} NMR ($CDCl_3$): 159.6, 148.7, 147.4, 137.7, 131.9 (q, J_{CF} = 34 Hz), 128.0 (q, J_{CF} = 4 Hz), 123.9, 122.7 (q, J_{CF} = 273 Hz), 122.3 (poorly resolved sept, J_{CF} = 4 Hz), 122.2, 79.9. ^{19}F NMR ($CDCl_3$): δ −63.2. Anal. Calcd for $C_{22}H_{11}F_{12}NO$: C, 49.55; H, 2.08; N, 2.63. Found: C, 49.61; H, 1.87; N, 2.62.

{pyC(4-^{t}Bu−C$_6$H$_4$)$_2$O}$_2$Ti(NMe$_2$)$_2$ (2a). A solution of bis(4-*tert*-butylphenyl)-2-pyridylmethanol (**1a**, 0.560 g, 1.50 mmol) in toluene (20 mL) was added dropwise at room temperature to a solution of Ti(NMe$_2$)$_4$ (0.168 g, 0.750 mmol) in toluene (20 mL). The deep red solution was stirred for 1 h, and the volatiles were removed under vacuum. The deep red solid was washed with pentane, dried under vacuum, and crystallized by slow evaporation of a dichloromethane solution under nitrogen purge. Yield 0.650 g, 98%; red rectangular crystals. ^{1}H NMR (CD_2Cl_2): δ 7.39 (d, J = 4.7 Hz, 2H), 7.33 (td, J = 7.9, 1.6 Hz, 2H), 7.25 (br m, 16H), 7.05 (d, J = 7.9 Hz, 2H), 6.36 (m, 2H), 3.31 (s, 12H), 1.34 (s, 36H). ^{1}H NMR (CD_2Cl_2, −30 °C): 7.36 (m, 8H), 7.27 (m, 8H), 7.09 (d, J = 8.3 Hz, 4H), 6.94 (d, J = 7.7 Hz, 2H), 6.30 (t, J = 6 Hz, 2H), 3.37 (s, 12H), 1.41 (s, 18H), 1.27 (s, 18H). ^{13}C{^{1}H} NMR (CD_2Cl_2): 168.0, 149.8, 148.8, 147.5 (v br), 135.9, 128.4, 124.8, 123.8, 120.9, 93.7, 49.1, 34.7, 31.6. Anal. Calcd for $C_{56}H_{72}N_4O_2Ti$: C, 76.34; H, 8.24; N, 6.36. Found: C, 76.24; H, 8.25; N, 6.40.

{9-(2-pyridyl)-9-fluorenolato}$_2$Ti(NMe$_2$)$_2$ (2b). A solution of 9-(2-pyridyl)-9-fluorenol (**1b**, 0.500 g, 1.93 mmol) in toluene (20 mL) was added dropwise to a solution of Ti(NMe$_2$)$_4$ (0.216 g, 0.964 mmol) in toluene (20 mL) at room temperature over 30 min. The deep red solution was stirred for 1 h, and the volatiles were removed under vacuum. The red solid was washed several times with pentane, dried overnight in vacuo, and recrystallized from toluene/pentane (10/1), yielding red rectangular crystals (0.552 g, 88%). The crude product was also recrystallized from dichloromethane/toluene (1/1), yielding red rectangular crystals suitable for X-ray diffraction. ^{1}H NMR (CD_2Cl_2): δ 9.01 (d, J = 5.0 Hz, 2H), 7.76 (d, J = 7.5 Hz, 4H), 7.44 (t, J = 7.8 Hz, 2H), 7.40 (t, J = 7.0 Hz, 4H), 7.17 (m due to overlapping t and d, 6H), 7.04 (d, J = 7.5 Hz, 4H), 6.46 (d, J = 7.9 Hz, 2H), 3.24 (s, 12H). ^{13}C{^{1}H} NMR (CD_2Cl_2): 168.3, 152.8, 150.0, 140.4, 138.0, 128.9, 128.2, 126.1, 121.7, 120.7, 120.2, 96.4, 48.9. Anal. Calcd for $C_{40}H_{36}N_4O_2Ti$: C, 73.62; H, 5.56; N, 8.58. Found: C, 73.68; H, 5.76; N, 8.30.

{pyC(3-CF$_3$−C$_6$H$_4$)$_2$O}$_2$Ti(NMe$_2$)$_2$ (2c). A solution of bis(3-(trifluoromethyl)phenyl)-2-pyridylmethanol (**1c**, 0.532 g, 1.34 mmol) in toluene (20 mL) was added dropwise at room temperature to a solution of Ti(NMe$_2$)$_4$ (0.150 g, 0.669 mmol) in toluene (15 mL). The solution was stirred for 1 h, and the volatiles were removed under vacuum. The deep red solid was washed with pentane, dried overnight under vacuum, and dissolved in dichloromethane. The solution was evaporated to dryness under nitrogen purge yielding a red viscous oil (quantitative yield). ^{1}H NMR (CD_2Cl_2): δ 7.6−7.4 (br m, 20H), 7.14 (d, J = 6 Hz, 2H), 6.56 (t, J = 6 Hz, 2H), 3.20 (s, 12H). ^{1}H NMR (CD_2Cl_2, −80 °C): 7.98 (s, 2H), 7.6 (m, 6H), 7.49 (m, 4H), 7.39 (m, 4H), 7.10 (d, J = 5.2 Hz, 2H), 6.94 (d, J = 8.0 Hz, 2H), 6.76 (s, 2H), 6.42 (t, J = 6.5 Hz, 2H), 3.21 (s, 12H). ^{13}C{^{1}H} NMR (CD_2Cl_2): 166.1, 151.0, 148.4, 137.1, 132.4 (br), 130.3 (q, J_{CF} = 32 Hz), 128.9, 125.1 (poorly resolved q, J = 4 Hz), 124.7 (q, J_{CF} = 272 Hz), 124.3 (poorly resolved q, J = 4 Hz), 123.7, 121.9, 93.2, 48.8. ^{19}F NMR (CD_2Cl_2): δ −62.6. Anal. Calcd for $C_{44}H_{36}F_{12}N_4O_2Ti$: C, 56.91; H, 3.91; N, 6.03. Found: C, 56.87; H, 3.85; N, 6.03.

{pyC(4-Ph−C$_6$H$_4$)$_2$O}$_2$Ti(NMe$_2$)$_2$ (2d). A solution of bis(4-phenylphenyl)-2-pyridylmethanol (**1d**, 0.517 g, 1.25 mmol) in benzene (20 mL) was added dropwise at room temperature to a solution of Ti(NMe$_2$)$_4$ (0.140 g, 0.625 mmol) in benzene (20 mL). The mixture was stirred for 1 h, and the volatiles were removed under vacuum. The deep red solid was recrystallized from hot toluene, yielding red crystals (0.493 g, 82%). ^{1}H NMR (C_6D_6): δ 7.82 (d, J = 4.9 Hz, 2H), 7.7 (br m, 24H), 7.24 (t, J = 7.4 Hz, 8H), 7.14 (t, J = 7.5 Hz, 4H), 7.03 (d, J = 8.0 Hz, 2H), 6.63 (td, J = 7.7, 1.5 Hz, 2H), 6.18 (t, J = 6.6 Hz, 2H), 3.86 (s, 12H). ^{13}C{^{1}H} NMR (CD_2Cl_2): 167.5, 149.7 (br), 148.9, 141.2, 139.9, 136.4, 129.3, 129.2, 127.6, 127.3, 126.8, 123.9, 121.3, 93.8, 49.2. Anal. Calcd for $C_{64}H_{56}N_4O_2Ti$: C, 79.99; H, 5.87; N, 5.83. Found: C, 79.82; H, 5.86; N, 5.63.

{pyC(4-NEt$_2$−C$_6$H$_4$)$_2$O}$_2$Ti(NMe$_2$)$_2$ (2e). A solution of bis(4-(diethylamino)phenyl)-2-pyridylmethanol (**1e**, 0.500 g, 1.24 mmol) in toluene (20 mL) was added dropwise to a solution of Ti(NMe$_2$)$_4$ (0.139 g, 0.620 mmol) in toluene (15 mL) at room temperature over 30 min. The deep red solution was stirred for 1 h, and the volatiles were removed under vacuum. The red solid was washed several times with pentane, dried overnight under vacuum, and recrystallized from ether. Yield 0.553 g, 95%; red microcrystals. Recrystallization of the crude product from toluene/pentane (1/1) yielded red rectangular crystals of **2e**·toluene suitable for X-ray diffraction. ^{1}H NMR (CD_2Cl_2): δ 7.50 (d, J = 4.6 Hz, 2H), 7.30 (td, J = 7.9, 1.7 Hz, 2H), 7.18 (very br m, 8H), 7.01 (d, J = 7.9 Hz, 2H), 6.56 (d, J = 9.0 Hz, 8H), 6.40 (m, 2H), 3.37 (q, J = 7.0 Hz, 16H), 3.31 (s, 12H), 1.17 (t, J = 7.0 Hz, 24H). ^{13}C{^{1}H} NMR (CD_2Cl_2): 169.2, 148.8, 146.7, 137.8 (br), 135.4, 129.8 (br), 123.6, 120.4, 111.0, 93.5, 49.1, 44.7, 12.8. Anal. Calcd for $C_{56}H_{76}N_8O_2Ti$: C, 71.47; H, 8.14; N, 11.91. Found: C, 71.58; H, 8.35; N, 11.40.

{11-(2-pyridyl)dibenzosuberolato}$_2$Ti(NMe$_2$)$_2$ (2f). A solution of 11-(2-pyridyl)dibenzosuberol (0.575 g, 2.00 mmol) in toluene (20 mL) was added dropwise to a solution of Ti(NMe$_2$)$_4$ (0.228 g, 1.00 mmol) in toluene (20 mL) at room temperature. The resulting deep red solution was stirred for 1 h at room temperature. The volatiles were removed under vacuum to give a red solid, which was washed with pentane (40 mL). This product was recrystallized from dichloromethane, washed with pentane, and dried under vacuum (0.41 g, 55%). ^{1}H NMR (CD_2Cl_2, 20 °C): δ 7.62 (d, J = 4.7 Hz, 2H), 7.46 (td, J = 7.9, 1.7 Hz, 2H), 7.25 (d, J = 7.2 Hz, 4H), 7.13 (t, J = 7.5 Hz, 4H), 7.01 (d, J = 8.1 Hz, 2H), 6.76 (m, 4H), 6.67 (m, 2H), 6.17 (d, J = 8.0 Hz, 4H), 4.12 (m, 4H), 3.07 (m, 4H), 2.73 (s, 12H, NMe$_2$). ^{1}H NMR (CD_2Cl_2, −75 °C): δ 7.37 (m, 4H), 7.23−7.17 (m, 4H), 7.09 (d, J = 7.4 Hz, 2H), 7.01 (t, J = 7.3 Hz, 2H), 6.81 (d, J = 7.9 Hz, 2H), 6.74 (t, J = 7.8 Hz, 2H), 6.64 (t, J = 7.9 Hz, 2H), 6.54 (t, J = 6.6 Hz, 2H), 6.04 (d, J = 8.1 Hz, 2H), 5.88 (d, J = 7.9 Hz, 2H), 4.22−4.14 (m, 2H), 3.52−3.45 (m, 2H), 3.10−2.99 (m, 4H), 2.80 (s, 12H, NMe$_2$). ^{13}C{^{1}H} NMR (CD_2Cl_2, 20 °C): 161.2, 148.6, 135.0, 131.1, 130.6, 127.2, 126.1, 125.2, 125.1, 121.5, 47.3 (NMe$_2$), 35.7; the *C*OTi resonance was not detected. Anal. Calcd for $C_{44}H_{44}N_4O_2Ti$: C, 74.62; H, 6.26; N, 7.91. Found: C, 74.41; H, 6.24; N, 7.73.

{pyC(3,5-(CF$_3$)$_2$−C$_6$H$_3$)$_2$O}$_2$Ti(NMe$_2$)$_2$ (2g). A solution of bis(3,5-bis((trifluoromethyl)phenyl)-2-pyridylmethanol (0.715

g, 1.34 mmol) in toluene (20 mL) was added dropwise to a solution of $Ti(NMe_2)_4$ (0.228 g, 1.00 mmol) in toluene (20 mL) at room temperature. The deep red solution was stirred for 1 h at room temperature. The volatiles were removed under vacuum to give a red solid, which was washed with pentane (40 mL). Recrystallization from toluene gave a dark red crystals (plates), which were separated by decantation, washed with pentane, and dried under vacuum (0.47 g, 59%). ^{1}H NMR (CD_2Cl_2, 20 °C): δ 7.89 (s, 4H), 7.80 (br s, 8H), 7.65−7.61 (m, 4H), 7.19 (d, J = 7.9 Hz, 2H), 6.76 (t, J = 6.3 Hz, 2H), 3.11 (s, 12H, NMe_2), ^{1}H NMR (CD_2Cl_2, −60 °C): δ 8.02 (s, 4H), 7.94 (s, 2H), 7.83 (s, 2H), 7.56 (t, J = 7.9 Hz, 2H), 7.43 (s, 4H), 7.31 (d, J = 5.0 Hz, 2H), 7.09 (d, J = 8.0 Hz, 2H), 6.62 (t, J = 6.3 Hz, 2H), 3.11 (s, 12H, NMe_2). ^{13}C{^{1}H} NMR (CD_2Cl_2): 164.7, 151.8, 148.3, 138.3, 131.8 (q, J_{CF} = 34 Hz), 128.6 (q, J_{CF} = 4 Hz), 123.9, 123.8 (q, J_{CF} = 274 Hz), 122.9, 122.0 (poorly resolved sept, J_{CF} = 4 Hz), 92.3, 48.4 (NMe_2). ^{19}F NMR (CD_2Cl_2): δ −63.1. Anal. Calcd for $C_{48}H_{32}F_{24}N_4O_2Ti$: C, 48.02; H, 2.69; N, 4.67. Found: C, 47.89; H, 2.51; N, 4.43.

{pyC(4-^{t}Bu−C_6H_4)$_2$O}$_2$Zr(NMe$_2$)$_2$ (3a). This compound was prepared according to the procedure for **2a** and crystallized by slow evaporation of a dichloromethane/toluene (10/1) solution under nitrogen purge. Yield 0.625 g, 92%, yellow crystals. ^{1}H NMR (CD_2Cl_2): δ 7.40 (td, J = 7.8, 1.5 Hz, 2H), 7.35 (d, J = 5.4 Hz, 2H), 7.31−7.17 (br m, 16H), 7.12 (d, J = 8.0 Hz, 2H), 6.45 (m, 2H), 3.02 (s, 12H), 1.35 (s, 36H). ^{1}H NMR (CD_2Cl_2, −40 °C): 7.44 (d, J = 8.2 Hz, 2H), 7.36 (td, J = 6.3 Hz, 1.5 Hz, 2H), 7.29 (br m, 12H), 7.13 (d, J = 5.4 Hz, 2H), 7.00 (d, J = 7.9 Hz, 4H), 6.36 (t, J = 6.4 Hz, 2H), 3.00 (s, 12H), 1.37 (s, 18H), 1.24 (s, 18H). ^{13}C{^{1}H} NMR (CD_2Cl_2): 169.3, 149.9, 147.2, 136.6, 128.1, 125.0, 124.5, 121.3, 91.6, 44.7, 34.7, 31.6. Anal. Calcd for $C_{56}H_{72}N_4O_2Zr$: C, 74.04; H, 7.99; N, 6.17. Found: C, 73.77; H, 7.96; N, 5.90.

{9-(2-pyridyl)-9-fluorenolato}$_2$Zr(NMe$_2$)$_2$ (3b). A solution of **1b** (0.500 g, 1.93 mmol) in toluene (20 mL) was added dropwise to a solution of $Zr(NMe_2)_4$ (0.258 g, 0.965 mmol) in toluene (20 mL) at room temperature over 30 min. The reaction mixture was refluxed for 1 h. The volatiles were removed under vacuum, and the yellow solid was washed with pentane. Recrystallization from toluene/pentane (10/1) yielded needles which collapsed to a yellow powder upon isolation. Yield 0.446 g, 67%. ^{1}H NMR (CD_2Cl_2): δ 8.90 (d, J = 5.4 Hz, 2H), 7.76 (d, J = 7.5 Hz, 4H), 7.50 (td, J = 7.9, 1.7 Hz, 2H), 7.39 (td, J = 7.5, 1.2 Hz, 4H), 7.22−7.15 (m, 6H), 7.08 (d, J = 7.5 Hz, 4H), 6.52 (d, J = 8.0 Hz, 2H), 2.94 (s, 12H). ^{13}C{^{1}H} NMR (CD_2Cl_2): 169.7, 152.6, 149.5, 140.3, 138.7, 129.0, 128.5, 125.3, 122.2, 121.7, 120.3, 44.5; alkoxide carbon not observed. Anal. Calcd for $C_{40}H_{36}N_4O_2Zr$: C, 69.03; H, 5.21; N, 8.05. Found: C, 68.89; H, 5.42; N, 7.79.

{pyC(4-NEt$_2$−C_6H_4)$_2$O}$_2$Zr(NMe$_2$)$_2$ (3e). This compound was prepared by the reaction of **1e** (0.500 g, 1.24 mmol) and $Zr(NMe_2)_4$ (0.166 g, 0.620 mmol) according to the procedure for **2e**, but with benzene as a solvent. The product was recrystallized from ether. Yield 0.376 g, 62%; yellow needles. ^{1}H NMR (C_6D_6): δ 7.91 (d, J = 5.1 Hz, 2H), 7.6 (br s, 8H), 7.20 (d, J = 8.0 Hz, 2H), 6.76 (td, J = 7.6 Hz, 1.5 Hz, 2H), 6.54 (br, 8H), 6.35 (t, J = 6.6 Hz, 2H), 3.70 (s, 12H), 2.99 (q, J = 7.0 Hz, 16H), 0.89 (t, J = 7.0 Hz, 24H). ^{13}C{^{1}H} NMR (C_6D_6): 171.2, 148.9, 146.7, 138.7, 135.5, 130.0, 124.6, 120.5, 111.6, 91.8, 45.7, 44.5, 12.9. Anal. Calcd for $C_{56}H_{76}N_8O_2Zr$: C, 68.32; H, 7.78; N, 11.38. Found: C, 68.41; H, 7.64: N, 11.14.

{pyC(3-CF$_3$−C_6H_4)$_2$O}$_3$Zr(NMe$_2$) (4c). This compound was prepared by the reaction of $Zr(NMe_2)_4$ (0.200 g, 0.748 mmol) and **1c** (0.890 g, 2.24 mmol) according to the procedure for **2c**. The crude product was recrystallized from toluene/pentane (10/1). Yield 0.644 g, 65%; pale yellow rectangular crystals. ^{1}H NMR (CD_2Cl_2): δ 8.25 (br, 3H), 7.53−7.48 (m, 9H), 7.40 (d, J = 8.5 Hz, 6H), 7.28 (d, J = 7.9 Hz, 6H), 7.24−7.17 (m, 9H), 6.72 (t, J = 5.9 Hz, 3H), 2.47 (s, 6H). ^{13}C{^{1}H} NMR (CD_2Cl_2): 167.4, 150.9, 148.1, 137.3, 132.1, 129.9 (q, J_{CF} = 32 Hz), 128.3, 125.2 (poorly resolved q, J = 4 Hz), 124.6 (q, J_{CF} = 273 Hz), 124.0, 123.9 (poorly resolved q, J = 4 Hz), 122.2, 91.3, 44.3. ^{19}F NMR (CD_2Cl_2): δ −62.6. Anal. Calcd for $C_{62}H_{42}F_{18}N_4O_3Zr$: C, 56.24; H, 3.20; N, 4.23. Found: C, 56.45; H, 3.30; N, 4.17.

{pyC(4-NEt$_2$−C_6H_4)$_2$O}$_4$Zr (5e). A solution of **1e** (0.240 g, 0.595 mmol) in benzene (15 mL) was added dropwise at room temperature to a solution of $Zr(NMe_2)_4$ (0.040 g, 0.149 mmol) in benzene (10 mL). The solution was stirred for 1 h. Removal of the volatiles under vacuum yielded a tan oil in quantitative yield. ^{1}H NMR (C_6D_6): δ 8.15 (d, J = 7.8 Hz, 4H), 8.07 (d, J = 4.6 Hz, 4H), 7.59 (d, J = 8.8 Hz, 16H), 7.10 (td, J = 7.7, 1.7 Hz, 4H), 6.35 (t, J = 5.7 Hz, 4H), 6.29 (d, J = 8.9 Hz, 16H), 2.99 (q, J = 7.0 Hz, 32H), 0.90 (t, J = 6.9 Hz, 48H). ^{13}C{^{1}H} NMR (C_6D_6): 170.6, 148.4, 146.1, 138.9, 135.3, 130.3, 123.9, 120.4, 111.3, 90.7, 44.4, 12.9. Anal. Calcd for $C_{104}H_{128}N_{12}O_4Zr$: C, 73.42; H, 7.58; N, 9.88. Found: C, 73.48; H, 7.49; N, 9.69.

{pyC(4-^{t}Bu−C_6H_4)$_2$O}$_2$Hf(NMe$_2$)$_2$ (6a). This compound was prepared according to the procedure for **2a** and crystallized by slow evaporation of dichloromethane/toluene (10/1) under nitrogen purge. Yield 0.684 g, 92%; pale yellow microcrystals. ^{1}H NMR (CD_2Cl_2): δ 7.41 (td, J = 7.9 Hz, 0.9 Hz, 2H), 7.36 (d, J = 5.4 Hz, 2H), 7.31 (d, J = 8.2 Hz, 8H), 7.2 (br s, 8H), 7.13 (d, J = 8.0 Hz, 2H), 6.44 (m, 2H), 3.06 (s, 12H), 1.32 (s, 36H). ^{1}H NMR (CD_2Cl_2, −20 °C): 7.39 (td, J = 8, 1.4 Hz, 2H), 7.3 (m due to three overlapping d, 14H), 7.06 (d, J = 8 Hz, 2H), 7.00 (d, J = 8 Hz, 4H), 6.39 (m, 2H), 3.06 (s, 12H), 1.38 (s, 18H), 1.26 (s, 18H). ^{13}C{^{1}H} NMR (CD_2Cl_2): 169.7, 150.0, 148.7, 147.5 (v br), 136.7, 128.2 (br), 125.0, 124.8, 121.4, 91.7, 44.7, 34.7, 31.6.

{pyC(4-NEt$_2$−C_6H_4)$_2$O}$_2$Hf(NMe$_2$)$_2$ (6e). A solution of **1e** (0.500 g, 1.24 mmol) in benzene (20 mL) was added dropwise at room temperature to a solution of $Hf(NMe_2)_4$ (0.220 g, 0.620 mmol) in benzene (20 mL). The yellow solution was stirred for 1 h, and the volatiles were removed under vacuum. The yellow solid was washed several times with pentane, dried overnight under vacuum, and recrystallized from ether. Yield 0.382 g, 58%; yellow needles. ^{1}H NMR (CD_2Cl_2): δ 7.45 (d, J = 5 Hz, 2H), 7.37 (t, J = 8 Hz, 2H), 7.1 (v br s, 8H), 7.10 (d, J = 8 Hz, 2H), 6.54 (d, J = 8 Hz, 8H), 6.47 (t, J = 6 Hz, 2H), 3.33 (q, J = 7.0 Hz, 16H), 3.03 (s, 12H), 1.10 (t, J = 7.0 Hz, 24H). ^{1}H NMR (CD_2Cl_2, −50 °C): δ 7.36 (t, J = 8 Hz, 2H), 7.24 (d, J = 6 Hz, 2H), 7.16 (d, J = 9 Hz, 4H), 6.97 (d, J = 8 Hz, 2H), 6.80 (d, J = 9 Hz, 4H), 6.48 (d, J = 9 Hz, 4H), 6.47 (d, J = 9 Hz, 4H), 6.40 (t, J = 6 Hz, 2H), 3.3 (m, 16H), 3.01 (s, 12H), 1.13 (t, J = 7 Hz, 12H), 1.05 (t, J = 7 Hz, 12H). ^{13}C-{^{1}H} NMR (C_6D_6): 171.6, 149.0, 146.7, 139.0, 135.6, 130.0 (br), 124.8, 120.6, 111.7 (br), 92.0, 45.7, 44.5, 12.8. Anal. Calcd for $C_{56}H_{76}N_8O_2Hf$: C, 62.76; H, 7.15; N, 10.46. Found: C, 66.85; H, 7.45; N, 9.59.

{9-(2-pyridyl)-9-fluorenolato}$_3$Hf(NMe$_2$) (7b). A solution of **1b** (0.500 g, 1.93 mmol) in toluene (20 mL) was added to a solution of $Hf(NMe_2)_4$ (0.228 g, 0.643 mmol) in toluene (20 mL) at room temperature over 30 min. The reaction mixture was refluxed for 2 h and evaporated to dryness under vacuum. The yellow solid was washed with pentane and dried. Recrystallization from hot toluene yielded pale yellow microcrystals. Yield 0.406 g, 54%. ^{1}H NMR (C_6D_6): δ 8.89 (br s, 3H), 7.55 (d, J = 7.6 Hz, 6H), 7.29 (br d, J = 6.6 Hz, 6H), 7.12 (t, J = 7.9 Hz, 6H), 6.84 (t, J = 7.4 Hz, 6H), 6.59 (td, J = 7.8, 1.5 Hz, 3H), 6.43 (d, J = 7.9 Hz, 3H), 6.33 (t, J = 6.4 Hz, 3H), 3.33 (s, 6H). ^{13}C{^{1}H} NMR (C_6D_6): 171.1, 154.8, 149.2, 140.5, 137.3, 128.4, 128.2, 126.3, 121.9, 121.7, 119.9, 94.7, 46.9. Anal. Calcd for $C_{56}H_{42}N_4O_3Hf$: C, 67.43; H, 4.24; N, 5.62. Found: C, 66.98; H, 4.12; N, 4.72.

{pyC(3-CF$_3$−C_6H_4)$_2$O}$_3$Hf(NMe$_2$) (7c). A solution of **1c** (0.672 g, 1.69 mmol) in toluene (20 mL) was added dropwise at room temperature to a solution of $Hf(NMe_2)_4$ (0.200 g, 0.564 mmol) in toluene (15 mL). The solution was stirred for 1 h, and the volatiles were removed under vacuum. The yellow solid was washed with pentane and dried overnight under vacuum. The crude product was recrystallized from benzene. Yield 0.652 g, 82%; pale yellow needles. ^{1}H NMR (C_6D_6): δ

8.34 (br, 3H), 7.72 (s, 6H), 7.2 (m, 12H), 6.8 (m, 9H), 6.73 (td, J = 7.6, 1.5 Hz, 3H), 6.23 (t, J = 6.0 Hz, 3 H), 2.85 (s, 6H). $^{13}C\{^1H\}$ NMR (C_6D_6): 167.6, 151.3, 148.0, 137.1, 132.1, 130.4 (q, J_{CF} = 32 Hz), 128.3, 125.1 (poorly resolved q, J = 4 Hz), 124.9 (q, J_{CF} = 273 Hz), 124.0, 123.9 (poorly resolved q, J = 4.0 Hz), 121.9, 91.3, 44.6. ^{19}F NMR (CD_2Cl_2): δ −62.6. Anal. Calcd for $C_{62}H_{42}F_{18}N_4O_3Hf$: C, 52.76; H, 3.00; N, 3.97. Found: C, 52.86; H, 3.01; N, 3.80.

X-ray Crystallography. The X-ray analyses of **2b** and **2e** were performed by R. D.Rogers. The X-ray analysis of **3a** was performed by A. L. Rheingold and G. P. A. Yap. Details are provided in Table 1 and the Supporting Information.

2b: An orange single crystal of **2b** was mounted in a glass capillary flushed with Ar and transferred to the goniometer. The space group was determined to be either the centric *Pnma* or the acentric *Pna*2$_1$ from the systematic absences; the subsequent solution and refinement of the structure was carried out in the latter. The geometrically constrained H atoms were placed in calculated positions and allowed to ride on the bonded atom with $B = 1.2 \times U_{equiv}(C)$. Refinement of non-H atoms was carried out with anisotropic temperature factors. The available crystals for **2b** were very small, and eventually the data for this compound were collected on a 0.1 × 0.1 × 0.4 mm crystal. The scattering at room temperature was very weak, and the final refinement exhibited high thermal motion. The refinement of this compound was based on all data (observed as well as unobserved), and as a result, the final R values are high. Despite the high R values, the refinement proceeded without difficulty. The geometrical details are affected by higher than normal esd's, but the overall structure and atom connectivity are clear.

2e: An orange single crystal of **2e**·toluene was mounted in a glass capillary flushed with Ar and transferred to the goniometer. The space group was determined to be *P*2$_1$/*n* from the systematic absences. The geometrically constrained H atoms were placed in calculated positions and allowed to ride on the bonded atom with $B = 1.2 \times U_{equiv}(C)$. The methyl hydrogens were included as a rigid group with rotational freedom at the bonded carbon ($B = 1.2 \times U_{equiv}(C)$). Refinement of non-H atoms was carried out with anisotropic temperature factors. A high degree of thermal motion was noted in a number of atoms, especially the ethyl and methyl groups. While disorder is most likely present in all or some of these atoms, no suitable disorder model could be successfully developed and refined. In addition, the toluene solvent molecule showed a high degree of thermal motion; however, again no model could be successfully refined. As a result, the solvent molecule H atoms were not included in the final refinement.

3a: Crystals of **3a** containing 0.5 equiv of NMe_2H were obtained from the toluene reaction solution from the reaction of **1a** and Zr(NMe$_2$)$_4$. A suitable crystal was sectioned and mounted in a capillary under N_2. The systematic absences were uniquely consistent with the space group *P*2$_1$/*n*. The NMe_2H molecule was located in the asymmetric unit with 50% refined partial occupancy. The N, O, and Zr atoms were refined anisotropically, the C atoms were refined isotropically, and the H atoms were placed in idealized positions.

Ethylene Polymerization. Polymerization experiments were performed in a 250 mL Fischer−Porter bottle equipped with a mechanical stirrer and temperature probe. Data are summarized in Table 4. The Fischer−Porter bottle was charged with toluene (120 mL), Al(^{i}Bu)$_3$ (1 mL, 4.0 mmol), and the metal amide complex. MAO (Albemarle; 9.9% solution in toluene; 4.49 wt % total Al; 7.0 mmol Al) was added. The reaction mixture was heated to 43 °C, and the bottle was charged with ethylene (1 atm). The ethylene pressure was maintained at 1 atm during the polymerization. The polymerization was quenched after 1 h by injection of EtOH/1 M HCl. The polymer was collected by filtration, washed several times with EtOH, dried (70 °C, vacuum oven, overnight), and weighed. ^{13}C NMR, gel permeation chromatography (GPC), and differential scanning calorimetry (DSC) analyses of the polymer samples were carried out at the Yokkaich Research Center, Mitsubishi Petrochemical Co., Japan. For DSC analyses, samples were heated from 30 to 200 °C at 50 °C/min and cooled to 0 °C at 10 °C/min and the second trace (0 to 200 °C at 10 °C/min) was recorded.

Acknowledgment. This work was supported by the Department of Energy (Grant No. DE-FG02-88ER13935) and the Mitsubishi Chemical Corporation.

Supporting Information Available: Tables of crystal data and structural refinement, atomic coordinates, bond lengths and angles, anisotropic displacement parameters, and hydrogen coordinates for **2b**, **2e**, and **3a** (32 pages). Ordering information is given on any current masthead page.

OM970236K